# Improved single crystal growth methods for oxide materials by MBE, LPE and $\mu$ - PD techniques

Dae - Ho Yoon and Masahito Yoshizawa

*Department of Materials Science and Technology, Faculty of Engineering, Iwate University, Morioka 020, Japan*

# MBE, LPE와 $\mu$ - PD기술에 의한 산화물재료의 개선된 단결정 성장방법

윤대호, 吉澤 正人

岩手大學 공학부 재료물성공학과, 盛岡 020, 일본

Abstract   The growth processes of improved methods for MBE, LPE and $\mu$ -PD methods are discussed taking the oxide materials, especially those of Bi - Sr - Ca - Cu family, $LiNbO_3$ and $K_3Li_2Nb_5O_{15}$ family as examples. It is suggested that the crystal growth far from equilibrium including composition homogeneity has been achieved to satisfy in understanding and controlling the atomic interfaces.

요     약  분자선 에피텍시얼(MBE)법, 액상 에피텍시얼(LPE)법과 마이크로 인상($\mu$ -PD)법에 의한 단결정 성장에 있어서의 새로운 접근을 논의하였다. 재료로써는 Bi - Sr - Ca - Cu계, $LiNbO_3$와 $K_3Li_2Nb_5O_{15}$계의 산화물을 사용하였으며, 비평형영역으로 부터의 고품질(균일 조성 및 저결함 밀도) 결정성장은 원자수준의 계면제어에 의해 가능함을 고찰할 수 있었다.

## 1. Introduction

Among the electronic and/or electrooptic materials, the films and micro single crystals have considerable interest in the miniaturization and high efficiency of the devices [1 - 3]. Without doubt, the eminent progresses in the field of superlattice structured multi-

layer epitaxy led to realization of new devices concepts, like quantum wells, quantum wires or dots for the optoelectronics, thin film waveguides for the nonlinear optics or superconductor films, for example.

Recently, significant success was obtained in the development of blue-green light-emitting hetero-diodes such as (Zn, Cd)Se using molecular beam epitaxy (MBE) technique [4,5]. Also, the production of very high quality $LiNbO_3$ films using liquid phase epitaxial (LPE) technique that film growth can be achieved at a much lower temperature than melting point [6] has been reported not long ago [7]. Moreover, it should not be forgotten that the conventional bulk growth technologies are still characterized by greatest material losses during crystal machining and wafer preparation that require new unconventional steps toward "in situ" shape tailoring during the growth process. In priority, the modern nonlinear optics needs crystals which are accommodated to the diameter and processing length of the laser beam to be modulated most efficiently [8]. Finally, it has been shown that the defect density (dislocations, multi-domains, cracks, chemical inhomogeneities) decreases rapidly with reduction of the crystal of the crystal diameter up to micro-dimensions and increasing crystallization velocity [9].

In this paper, the improved crystal growth methods of oxide film and micro single crystals are focused with special consideration of the consequences of an incongruent melt on compositional homogeneity. The first procedure employed to control the surface atomic

layer during the growth was MBE growth method. Also, films of higher crystalline quality was grown using a new LPE technique. Next, special attention was concentrated to investigate the growth of micro single crystals by the micro-pulling down ($\mu$-PD) method.

## 2. Bi-Sr-Ca-Cu-O thin films grown by MBE method

Molecular beam epitaxy (MBE) with in situ observation by reflection high-energy electron diffraction (RHEED) is a key technology for controlled layered growth on the atomic scale in manufacturing of thin films. Thin film superconducting devices and by the prospect of artificial layering of these materials has led to renewed interest for MBE growth to develop techniques ever since the discovery of the high superconducting copper oxides in 1986. In the first attempts at MBE [10] growth of oxide films of Cu, Dy and Ba with the aim of preparing the high $T_c$ phase $Dy_1Ba_2Cu_3O_{7-x}$. The oxygen flux at the substrate was controlled by leak valve and impinged on the substrate from a tube source. However, the films were insulating as-grown. Subsequent furnace annealing in flowing oxygen led to superconducting behavior.

Oxidation studies for MBE [11-13] have been investigated using more reactive form of oxygen, such as distilled ozone($O_3$), nitric dioxide gas ($NO_2$) and plasma-excited oxygen. However, it is not yet clear whether

oxide films of similar quality can be pre-pared. Oxide film epitaxy is clearly a complex growth process requiring precise control of oxygen beam flux background reactivity of impinging oxygen species. This field is still in its fancy and requires a careful approach of growth conditions on oxide film stoichiometry and perfection. To overcome these problems for our approach, the combination of radical oxygen source and MBE is used for the growth of Bi - oxide superconducting films.

The elementary stages in MBE are described in Fig. 1, in this experiment. Absorbed atoms or molecules are incorporated at the position where they arrived. They dif-
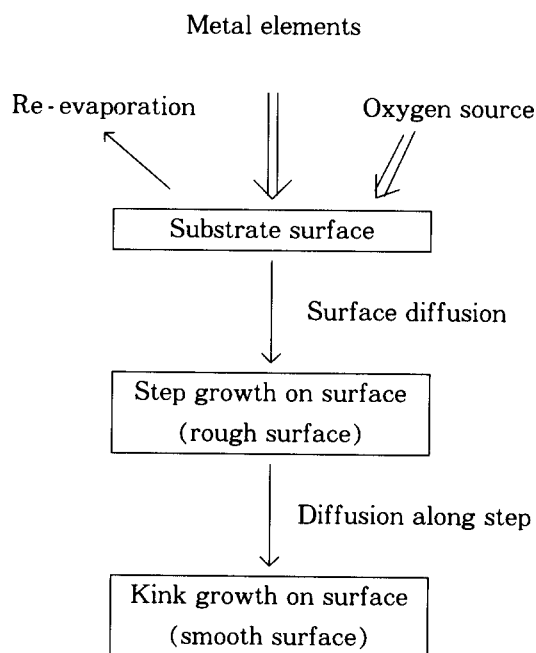
Metal elements

Re - evaporation        Oxygen source

Substrate surface

Surface diffusion

Step growth on surface
(rough surface)

Diffusion along step

Kink growth on surface
(smooth surface)

Fig. 1. Elementary stages in oxide MBE growth.

fuse until entering the steps which are mostly originated from 2 - dimensional (2D) nuclei or a misoriented substrate. The entering atoms move along the step to find a kink having a smooth surface. Thin films are grown using RHEED patterns compiled during and after the growth of Bi - oxide superconductor. The RHEED picture with the positions at which the intensity variation result in the growth by 2D layer growth was measured. During growth the phase of the RHEED pictures differed among the observed points. These data of the RHEED patterns suggest a rough - and - flat transition by nucleation and surface diffusion during the growth process.

The MBE method used is described in Ref. 14. Knudsen - cells (K - cells) were used to provide the molecular beams of Bi, Sr, Ca and Cu. The cell material was PBN (pyrolytic boron nitride). The evaporation rates from each cell were measured with a quartz crystal thickness monitor at the substrate position. This monitor was kept away from the substrate (MgO or $SrTiO_3$) during growth process. The base pressure was $1 \times 10^{-9}$ Torr. Oxidation was provided by a flux density of activated oxygen from an rf - excited discharge (coil type generator) introducing oxygen through a leak valve. Corresponding to the oxygen flow rate, the pressure of the system ranged from $1 \times 10^{-5}$ Torr to $1 \times 10^{-4}$ Torr. Figure 2a shows a schematic diagram of this radical beam source, radio - frequency (13.56 MHz) plasma was used to activate oxygen.

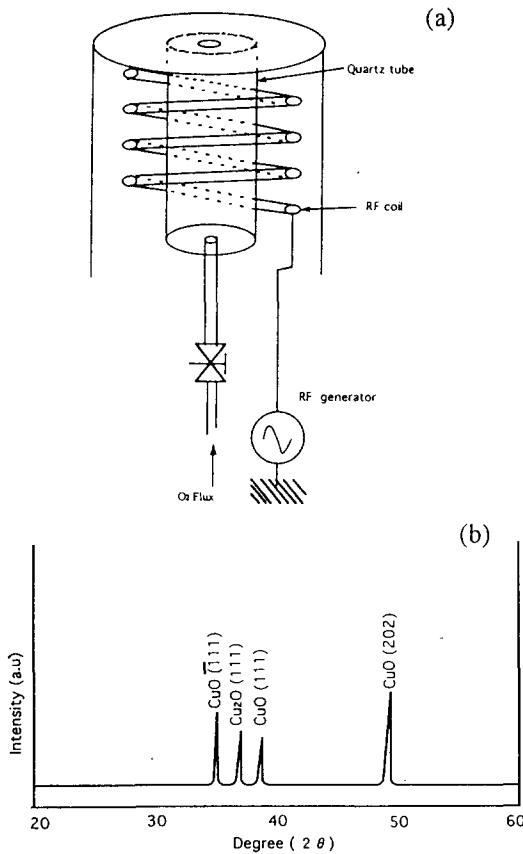Figure 2b shows the X - ray diffraction

(a)



(b)



Fig. 2. Schematic diagrams of the oxygen radical beam source (a), and the X-ray diffraction pattern of Cu-O film (b).

pattern of Cu-O film prepared by the radical conditions having 2 sccm oxygen flow rate and 150 W rf power. Evaporation rate of Cu was $0.6 Å/s$, substrate temperature was 700℃. It can be seen that Cu oxide was well formed the mentioned conditions. The number of activated oxygen species changed as the rf power and oxygen flow rate. Further, the synthesis of Bi-oxide superconductors was achieved by coevaporated or shutter-controlled growth of each metal ele-

ments (Bi, Sr, Ca and Cu) during the flow of radical oxygen at the substrate temperature of 700℃. In this way a Bi-oxide layered structure (the growth is controlled on the atomic scale) was prepared on a basal-plane MgO or $SrTiO_3$ substrate. The obtained results of oxidation and superconductivity need to consider in detail. The detailed correlation between oxidation and parameters for radical system or superconductivity will be reported in future.

## 3. $LiNbO_3$ films grown by LPE method

$LiNbO_3$ films with high crystalline quality have been attempted from a solid-liquid co-existing melt using a new liquid phase epitaxial (LPE) technique described in Ref. [15]. The films were grown on $LiNbO_3$ or $LiTaO_3$ substrates using a vertical dipping without substrate rotation. The melt was cooled below 925℃ and held more than 12 hours at this temperature. Although this led to the crucible wall being covered with solid $LiNbO_3$ generated by nucleation, the melt surface was in a completely uniform liquid phase. At this time, the liquid phase was in a saturated state at this temperature (formation of a solid-liquid coexisting melt), the substrate was dipped in the melt.

Figure 3 shows the difference of nucleation energies between conventional method and solid-liquid coexisting melt method. When film growth is performed by a conventional method from a uniform liquid phase melt, the substrate is the first solid phase
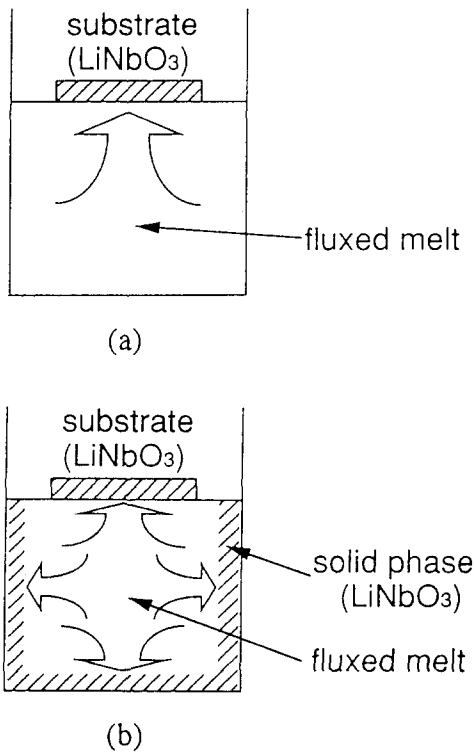
(a)



(b)

Fig. 3. Schemes of nucleation energies between conventional method (a), and solid - liquid coexisting melt method (b).

which contacts the liquid phase. Nucleation (film growth) occurs abruptly only at the substrate surface, because it is the lowest nucleation energy point in the system (Fig. 3a). On the other hand, when the film is grown from a solid - liquid coexisting melt, the liquid phase is already in contact with a solid phase (of the crucible wall) which is the same material as the substrate. In this case, the substrate is not the first such solid phase in the melt, and film growth can start smoothly under the same conditions as the coexisting solid phase (Fig. 3b). Therefore, with this technique, the reproducibility of

film properties such as film thickness can be better than with the conventional technique.

Figure 4 shows a schematic diagram of as - grown film on substrate and the change of X - ray rocking curve when the film was grown at 915℃ using the solid - liquid coexisting technique. LiNbO₃ films of higher crystalline quality (5.6 sec) than underlying LiNbO₃ substrates (6.8 sec) have been successfully grown. Also, the crystallinity of the epitaxial films can be better than that of the conventional LPE method because the degree of supercooling with the coexisting
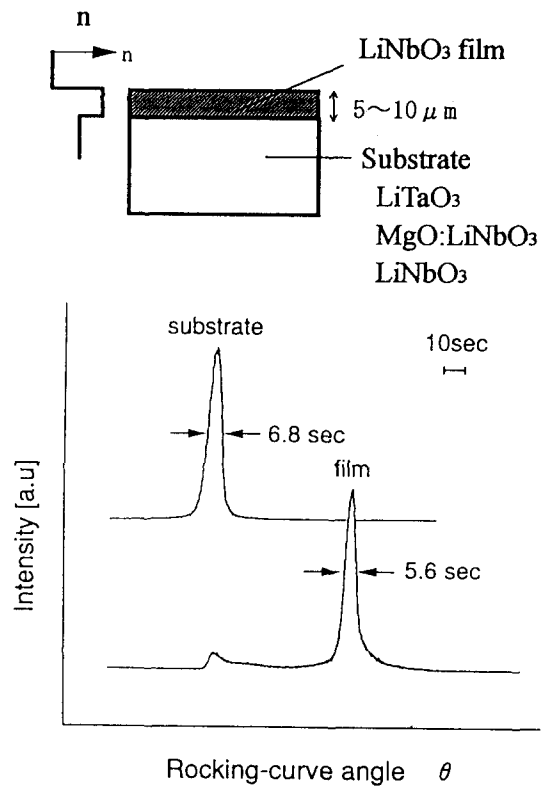


Fig. 4. Scheme of as - grown film on substrate and the results of X - ray rocking curve.

solid phase is not affected by changes in the melt composition. Furthermore, it has been found that the composition of the film can be controlled by changing the growth temperature, and the lattice mismatch along the c-axis saturates above the film thickness of 20 $\mu$m and decreases with increasing growth temperature.

## 4. LiNbO₃, KLN crystals grown by $\mu$-PD method

In large size single crystals high-quality alternative crystals have not yet been produced by conventional growth techniques. In contrast, in micro single crystals which are just device size with diameters below 1 mm, high-quality crystals with low defect density and composition homogeneity can be expected to produce by development a new growth process, the micro pulling down ($\mu$-PD) method [9,16].

Using the $\mu$-PD method, as shown in Fig. 5, crack-free LiNbO₃ micro single crystals have been grown with uniform diameters in the 60 $\mu$m to 800 $\mu$m range, independent of melt comosition (48.6, 50 and 58 mol %Li₂O). The downward growth of shaped crystals from a micro-nozzle, namely $\mu$-PD method, is characterized by a very large axial temperature gradient below the nozzle top (along the growing crystal) which yields about 200 ~ 300℃/mm [9]. It is well known from thermo-elastic dislocation theory [17] that such high gradient is not danger if nonlinearities and radial temperature differ-
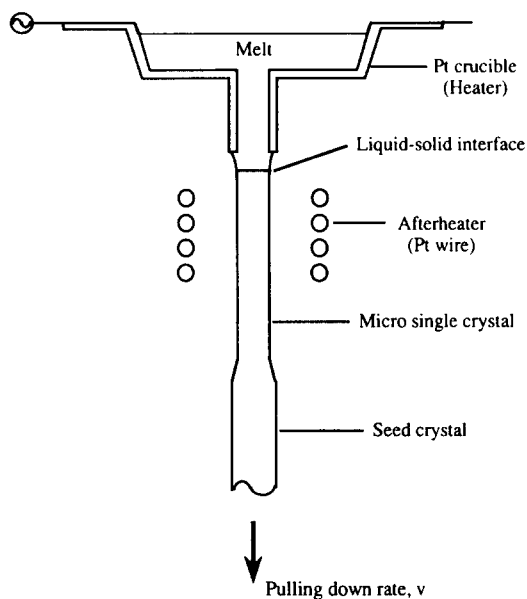


Fig. 5. Scheme of the $\mu$-PD method.

ences do not take place.

Very high pulling rate, v, is possible at $\mu$-PD method that follows from the thermal balances at the growing interface,

$$v = (K_s G_s - k_1 G_1)/\rho \cdot \Delta H$$

where $k_s$ and $k_1$ are the thermal conductivity in solid (s) and liquid (1), $G_s$ and $G_1$ are the temperature gradients, respectively, $\rho$ is the density and $\Delta H$ is the heat of fusion. At $G_s$ = 200℃/mm and near homogeneous temperature within the crucible and nozzle ($G_1 \approx$ 0), a maximum pulling rate of about 1 m/h can be estimated for LiNbO₃. In fact, the pulling rates between 30 and 120 mm/h were used successfully, much faster than that at conventional Czochralski (CZ) growth rates (usually $\leq$ 5 mm/h).

Voids, subgrain boundaries and disloca-

tions were not found in crystals having diameters of 500 $\mu$m or smaller for $LiNbO_3$ (Fig. 6). The homogeneous axial distribution of the chemical composition reflects an effective distribution coefficient of unity. Also, crack-free $K_3Li_{2-x}Nb_{5+x}O_{15+2x}$ (KLN) micro single crystals have been successfully grown by the $\mu$ -PD method, with high growth rates. Especially, no fractures normal to the c-axis have been observed after growth, unlike the cases of crystals grown by the top-seeded solution growth (TSSG) and CZ methods [18,19]. KLN crystals are of increasing interest due to the excellent second harmonic generation (SHG) characteristics suitable for conversion from red to blue wavelength [20]. The $\mu$ -PD grown crystals were applied for frequency doubling from 790 nm to 920 nm of a Ti : sapphire laser and (Ga, Al)As laser [21].
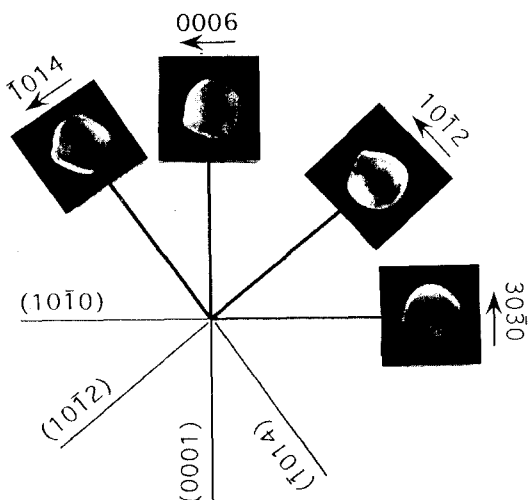
# 5. Conclusions

It was not possible to obtain homogeneous compositions with high quality from the top to the bottom of crystals grown from incongruent melt by the conventional growth methods. Using the MBE method, oxidation can be well formed by activated oxygen from a radical source, therefore oxide thin films can be controlled layered growth on the atomic scale. Also, films of higher crystalline quality than substrate can be grown by the LPE method with a solid-liquid coexisting melt. Crystals having a nearly homogeneous composition along the growth axis with high crystalline quality can be obtained independent of melt composition by the $\mu$ -PD method. The wide variety of the growth process available with MBE, LPE and $\mu$ -PD methods give it an advantage over more conventional approaches in understanding and controlling the development of atomic interfaces.

Fig. 6. X-ray topographs of a $\mu$ -PD crystal having diameter of 500 $\mu$m.

# References

[ 1 ] S. Kondo, S. Miyazawa, S. Fushimi and K. Sugii, Appl. Phys. Lett. 26 (1975) 489.

[ 2 ] S. Sudo, I. Yokohama, A. Cordova-

Plaza, M.M. Fejer and R.L. Byer, Appl. Phys. Lett. 56 (1990) 1931.

[ 3 ] H. Yoshinaga and K. Kitayama, Appl. Phys. Lett. 56 (1990) 1728.

[ 4 ] T. Matsumoto, T. Iwashita, K. Sakamoto and T. Kato, J. Crystal Growth 138 (1994) 63.

[ 5 ] S.Y. Wang, P. Thompson, G. Horsburgh, J.T. Mullins, I. Hauksson, K.A. Prior and B.C. Cavenett, J. Crystal Growth 138 (1994) 647.

[ 6 ] A.A. Ballman, H. Brown, P.K. Tien and S. Riva-Sanse-verino, J. Crystal Growth 29 (1975) 289.

[ 7 ] A. Yamada, H. Tamada and M. Saitoh, J. Crystal Growth 132 (1993) 48.

[ 8 ] T. Taniuchi, D.H. Yoon and T. Fukuda, Extended Abstracts (The 7th Meeting), J. Kor. Crystal Growth (1994) A05.

[ 9 ] D.H. Yoon, I. Yonenaga, T. Fukuda and N. Ohnishi, J. Crystal Growth 142 (1994) 339.

[10] C. Webb, S.L, Weng, J.N. Eckstein, N. Missert, K. Char, D.G. Schlom, E.S. Hellman, M.R. Beasley, A. Kapitulnik and J.S. Harris, Jr., Appl. Phys. Letters 51 (1987) 1191.

[11] Y. Nakayama, H. Ochimizu, A. Maeda, A. Kawazu, K. Uchinokura and S. Tanaka, Jpn. J. Appl. Phys. 28 (1989) L1217.

[12] S. Watanabe, M. Kasai and T. Hanada, Jpn, J. Appl. Phys. 29 (1990) L1111.

[13] Y. Ishzuka, Y. Terashima and T. Miura, Jpn. J. Appl. Phys. 29 (1990) L2045.

[14] D.H. Yoon, I. Agung, M. Oyama, H. Fujishiro and M. Yoshizawa, Jap. J. Crystal Growth 22 (1995) 221.

[15] T. Kawaguchi, D.H. Yoon, M. Minakada, Y. Okada, M. Imaeda and T. Fukuda, J. Crystal Growth 152 (1995) 87.

[16] D.H. Yoon and T. Fukuda, J. Kor. Crystal Growth 4 (1994) 405.

[17] B.K. Vainshtein, V.M. Fridkin and V. L. Indenbom, Modern Crystallography, Vol. 2, (Springer, Berlin, 1982).

[18] T. Fukuda, J. Crystal Growth 6 (19-70) 293.

[19] W.A. Bonner, W.H. Grodkiewicz and L.G. Van Uitert, J. Crystal Growth 1 (1967) 318.

[20] J.J.E. Reid, M. Ouwerkerk and L.J.A. M. Beckers, Philips J. Res. 46 (1992) 199.

[21] D.H. Yoon, M. Hashimoto and T. Fukuda, Jpn. J. Appl. Phys. 33 (1994) 3510.